

## Gamma Shielding Behavior of Zinc Doped Sodium Bismuth Borate Glass $x\text{ZnO}-(15-x)\text{Na}_2\text{O}-15\text{Bi}_2\text{O}_3-70\text{B}_2\text{O}_3$

<sup>1</sup>**Mohammed Abdullahi**, <sup>2</sup>**Abubakar Saddiq Dalhatu**, <sup>3</sup>**Aliyu Mohammed Aliyu**, <sup>3</sup>**Dauda Abubakar**,  
<sup>3</sup>**Auwal Baballe** and <sup>3</sup>**Umar Garba Musa**

<sup>1</sup>Department of Physics with Electronics, Auchi Polytechnic Auchi, Edo State, Nigeria.

<sup>2</sup>Department of Remedial Studies Federal University of Health and Nutrition Azare, Bauchi State, Nigeria.

<sup>3</sup>Department of Physics, Sa'adu Zungur University, Bauchi State, Nigeria.

\*Corresponding Author's Email: [abdullahimhammad478@gmail.com](mailto:abdullahimhammad478@gmail.com) Phone: +2348133316564

### ABSTRACT

The radiation shielding properties of zinc doped sodium bismuth borate glasses were analyzed using Phy-X/PSD. The chemical composition of glass  $x\text{ZnO}-(15-x)\text{Na}_2\text{O}-15\text{Bi}_2\text{O}_3-70\text{B}_2\text{O}_3$  with  $0 \leq x \leq 12$  mol % glass, and are coded as ZNBB1, ZNBB2, ZNBB3, ZNBB4, and ZNBB5 in increasing  $x\text{ZnO}$  content. Phy-X/PSD was used to determine the mass attenuation coefficient (MAC), linear attenuation coefficient (LAC), and half value layer (HVL), tenth value layer (TVL), and mean free path (MFP) of the investigated glasses. The maximum values for all the glasses can be observed at the lowest tested energy, 0.015 MeV and are equal to 27.017, 35.330, 42.036, 47.560, 52.190 ( $\text{cm}^2/\text{g}$ ) for the ZNBB1, ZNBB2, ZNBB3, ZNBB4, and ZNBB5 glasses, respectively. At this energy, the MAC of the glasses can be observed to increase as the Zinc oxide concentration of the sample increases, which is due to the increase in density that correlates with  $\text{B}_2\text{O}_3$  content. The minimum HVL values occurred at the lowest tested energy, 0.15 MeV, and decreased with decreasing energy, meaning that the glasses are more effective at lower energies. The results proved that the glass with the highest content of zinc oxide, has the higher density with greatest potential for radiation shielding applications.

**Keywords:**  
 Radiation,  
 Shielding,  
 Bismuth,  
 Borate,  
 Glass,  
 Density,  
 Energy.

### INTRODUCTION

Radiation is energy traveling through space, having some wave, and some particle characteristics. It can be categorized into 2- different kinds, ionizing and non-ionizing, which depend on the amount of energy present. Ionizing radiation can cause damage to matter, as it is capable of detaching electrons from atoms, and can be especially harmful to living tissue. This type of radiation mainly comes from the nuclei of atoms. Unstable nuclei often emit excess energy as radiation in the form of gamma photons. Gamma radiations represent energy transmitted in a wave without the movement of a medium. Gamma photons have relatively high energy and accordingly can move through the human body. Radiation has many advantageous applications, ranging from dental and medical fields to uses in agriculture, industry, and power generation (A.S. Abouhaswa et al., 2020). Studying the effect of ionizing radiation on matters becomes with an urgent consideration for researchers because of the harmful and destructive effects

of ionizing radiation on humans and environment. Lead and concrete are common effective ways to shield ionizing radiation to their safe limit that does not approximately affect matter (Abou Hussein et al., 2021). Lead has great mechanical and physical features which makes it an effective shielding material. However, the toxicity of lead and the harm it can cause to the environment and humans can be lethal, it also may produce small particles in the form of aerosols that may be swallowed or breathed in by humans and animals and concrete is opaque and needs a large area for installing. But the usage of concrete has several drawbacks due to its density and structural strength, which decreases with the water content, thereby directly affecting the calculated shielding parameters (E. Salama, et al. 2019). However, an alternative material can be used to achieve the same target, such as glass. From recent study, glass materials have gain attention in nuclear and radiation field as radiation shielding material, Glasses have dual properties because they are transparent to visible light

and they can attenuate gamma rays, thereby allowing their use as transparent radiation shields (E. Salama, et al., 2019). Glass materials have attracted many researchers' interests and have been used as a potential inorganic material for diverse applications such as optical fiber, optoelectronic devices, optical switch devices, radiation shielding. The current research has therefore shifted towards developing glass shields that possess high density and adequate transparency, aiming to replace conventional lead and concrete shielding alternative. The aim of this research is to evaluate the gamma shielding behavior of sodium Bismuth borate  $x\text{ZnO}-(15-x)\text{Na}_2\text{O}-15\text{Bi}_2\text{O}_3-70\text{B}_2\text{O}_3$  glass system doped with  $x = 0, 6, 8, 10$  and  $12$  mol% of  $\text{ZnO}$ .

## MATERIALS AND METHODS

This section explain the methodology that will be used in this research to fulfil the objective of the research. Sample preparation and sample analysis were performed based on the standard procedure. The Zinc sodium bismuth borate glasses doped with varying concentration of zinc oxide were prepared using melting quenching technique and Glass densities was measured by Archimedes method. The sample structure was determined by X-ray diffraction. The radiation shielding parameters such as mass attenuation coefficient (MAC), linear attenuation coefficient (LAC) of zinc oxide doped sodium bismuth borate glasses were obtained using computational software Phy-X/PSD. The mechanical properties of prepared glasses were determined using Makishima–Mackenzie model.

### Preparation of Glass

Five samples of borate/sodium/bismuth glasses doped with  $\text{ZnO}$  with chemical form  $x\text{ZnO}-(15-x)\text{Na}_2\text{O}$ -

$15\text{Bi}_2\text{O}_3-70\text{B}_2\text{O}_3$  with ( $x = 0, 6, 8, 10, 12$  mol%) glasses were selected. The raw materials of  $\text{ZnO}$ ,  $\text{Na}_2\text{PO}_4$ ,  $\text{Bi}_2\text{O}_3$  and  $\text{B}_2\text{O}_3$  were of analytic reagent (AR) grade. All the raw materials were weighed using electronic balance with precision of 1 mg and mixed together in pestle mortar with pestle and later put in alumina crucible. The alumina crucible was then placed in Muffle furnace at temperature with range 900–1000 °C and kept for 1 hour till a bubble free liquid was formed. The sample was poured in a preheated graphite mound and immediately transferred to annealing furnace kept at 400 °C for a period of 2 hours to remove internal stress. The glass sample formed after the annealing process was polished with sand papers of 1500, 1200 and 1000 grade and cerium oxide in order to acquire maximum flatness and smooth surface. Samples structures were studied at room temperature utilizing XRD spectroscopy (Bruker, AXS D8 Advance, Germany,  $\text{CuK}\alpha$  radiation). Glass samples densities ( $\rho$ ) glass were obtained utilizing Archimedes' method as in Eq. 1 employing toluene as an immersion liquid.

$$\rho_{\text{glass}} = \frac{W_a}{W_a - W_T} \rho_T \quad (1)$$

Where  $W_a$  and  $W_T$  are respectively the weight of the glass sample in air and toluene liquid.  $\rho_T$  denotes the toluene liquid mass density and equals to  $0.86 \text{ g/cm}^3$ . Also, the following equation was used to evaluate the molar volume  $V_m$  of the synthesized glasses:

$$V_m = \frac{M.W_{\text{glass}}}{\rho_{\text{glass}}} \quad (2)$$

The chemical composition, density, and molar volume of the synthesized samples are listed in Table 1. below. The optical measurements were applied to the polished glass discs utilizing JASCO UV–Vis–NIR spectrophotometer model V-570.

**Table 1: Nominal Composition  $x\text{ZnO}-(15-x)\text{Na}_2\text{O}-15\text{Bi}_2\text{O}_3-70\text{B}_2\text{O}_3$  Doped with Different Concentration of  $x\text{ZnO}$  ( $x = 0, 6, 8, 10$  and  $12$  in mol %)**

| S/N | Glass Code | $\text{ZnO}$ | $\text{Na}_2\text{O}$ | $\text{Bi}_2\text{O}_3$ | $\text{B}_2\text{O}_3$ | Density ( $\text{g/cm}^3$ ) | Molar Volume( $\text{cm}^3/\text{mol}$ ) |
|-----|------------|--------------|-----------------------|-------------------------|------------------------|-----------------------------|--|
| 1   | ZNBB1      | 0            | 15                    | 15                      | 70                     | 3.75                        | 34.04                                    |
| 2   | ZNBB2      | 6            | 9                     | 15                      | 70                     | 3.97                        | 32.50                                    |
| 3   | ZNBB3      | 8            | 7                     | 15                      | 70                     | 3.99                        | 32.37                                    |
| 4   | ZNBB4      | 10           | 5                     | 15                      | 70                     | 4.08                        | 31.81                                    |
| 5   | ZNBB5      | 12           | 3                     | 15                      | 70                     | 3.99                        | 31.38                                    |

### Phy-X / PSD Software

The Photon shielding and Dosimetry (Phy-X/PSD) database, accessible at <http://www.phy-x.com> enables calculation of gamma and neutron attenuation parameter for series of element. These parameter include: Linear Attenuation Coefficient, (LAC), Mass Attenuation Coefficient, (MAC), Effective Atomic Number, (Zeff), Half Value Layer, (HVL) Tenth Value Layer, (TVL), Mean Free Path, (MFP) and Removal Cross-Section. The glass system of  $x\text{ZnO}-(15-x)\text{Na}_2\text{O}-15\text{Bi}_2\text{O}_3-70\text{B}_2\text{O}_3$  has been fabricated by solid-state reaction, which is coded as

ZNBB1, ZNBB2, ZNBB3, ZNBB4 and ZNBB5 and the total details are displayed in Table 1. Meanwhile, the density of the ZNBB glass system is carried out to be  $3.75$ ,  $3.97$ ,  $3.99$ ,  $4.08$  and  $3.99 \text{ g/cm}^3$  corresponding to  $0$  mol%,  $6$  mol%,  $8$  mol%,  $10$  mol% and  $12$  mol% Zinc oxide. A series of radiation-shielding parameters consist of  $\mu$ ,  $\mu/\rho$ , the effective numbers (Zeff), the Half value layer (HVL), the tenth value layer (TVL), and the mean free paths (MFP), which can be derived by utilizing Phy-X/PSD database. Moreover, the energy range of this work is calculated by the software between  $15$  keV and

15 MeV. Meanwhile, it needs to choose the mole fraction, weight fraction, density of the materials, and radiation energy (15 keV-15 MeV or 1 KeV-100 GeV) for assessing the ability of radiation shielding (J.M. An et al., 2021). The software also includes some commonly known radioactive sources ( $^{22}\text{Na}$ ,  $^{55}\text{Fe}$ ,  $^{60}\text{Co}$ ,  $^{109}\text{Cd}$ ,  $^{131}\text{I}$ ,  $^{133}\text{Ba}$ ,  $^{137}\text{Cs}$ ,  $^{152}\text{Eu}$  and  $^{241}\text{Am}$ ) and their corresponding energies, as well as certain distinctive (K-shell) X-ray energies of Cu, Rb, Mo, Ag, Ba, and Tb elements that the user can choose from (Şakar et al., 2019).

To begin, it is essential to accurately define the composition of the material that will be used in the calculations. The software allows users to input the material composition in two different formats: mole fraction or weight fraction. Once the desired format is selected, users must ensure that the sum of the mole or weight fractions equals 100% or 1, and if necessary, normalize the values before entering them into the program. Furthermore, the density of the material in its phase state (in g/cm<sup>3</sup>) is required for calculating various shielding parameters, including LAC, HVL, TVL, and MFP. Additionally, users must enter the material label in the designated box to proceed with the calculations. The software has predefined two energy ranges: 15 keV to 15 MeV, which is relevant to the ANSI database and used for calculating the Exposure Air-Borne Fraction (EABF) and Exposure Buildup Factor (EBF), and 1 keV to 100 GeV. Additionally, the software includes a library of well-known radioactive sources, such as  $^{22}\text{Na}$ ,  $^{55}\text{Fe}$ ,  $^{60}\text{Co}$ ,  $^{109}\text{Cd}$ ,  $^{131}\text{I}$ ,  $^{133}\text{Ba}$ ,  $^{137}\text{Cs}$ ,  $^{152}\text{Eu}$ , and  $^{241}\text{Am}$ , along with their corresponding energies. The software also provides a selection of characteristic X-ray energies obtained from secondary sources, including the K-shell energies of various elements like Cu, Rb, Mo, Ag, Ba, and Tb. Users can easily select and utilize these predefined energy ranges and radioactive sources to facilitate their calculations and analyses.

The Mass Attenuation Coefficient (MAC) is a quantity that describes the interaction probability between gamma photons and the mass per unit area for a certain medium and can be calculated by the well-known Beer–Lambert. The parameter  $\mu$  (cm<sup>-1</sup>) of the incident gamma rays of the investigated glasses can be described using the Beer–Lambert relationship, which is shown in Eq. 3 below as reported by Jackson and Hawkes (1981).

$$I = I_0 e^{-\mu d} \quad (3)$$

The incident radiation intensity  $I_0$  decreases exponentially as the photons travel through the glass.  $I$  Represents the transmitted radiation intensity obtained after the photons pass through a glass of thickness  $d$ .  $\mu$  (cm<sup>-1</sup>) describes the interaction probability between the glass and the incident photons, which depends on  $d$ . The MAC (mass attenuation coefficient) ( $\mu_m$ , in cm<sup>2</sup>/g) depends on  $\mu$  (cm<sup>-1</sup>) and glass density  $\rho$  (g/cm<sup>3</sup>), as shown in Eq. 4.

$$\mu_m = \frac{\mu}{\rho} = \frac{\ln(I/I_0)}{\rho d} \quad (4)$$

The HVL (half value layer) and TVL (tenth value layer) given by Eq. 5 and 6. describe the thickness required to reduce photon intensity to 50% and 10% of its initial value, respectively (Şakar et al., 2020)

$$HVL = \frac{\ln 2}{\mu} = \frac{0.693}{\mu} \quad (5)$$

$$TVL = \frac{\ln 10}{\mu} = 2.302 \quad (6)$$

## RESULTS AND DISCUSSION

The structural and photon attenuation properties of a Sodium Bismuth Borate glasses doped with varying concentration of zinc oxide were theoretically analyzed within a specific energy range. Theoretical calculations were performed using Phy-X/PSD to determine the radiation shielding parameters, which including mass attenuation coefficient (MAC), linear attenuation coefficient (LAC), half-value layer (HVL) and tenth value layer (TVL) for gamma rays emitted by  $^{137}\text{Cs}$  and  $^{60}\text{Co}$  sources, spanning at energy range of 0.015 to 15 MeV. A comparative analysis of the radiation shielding parameters was then conducted for different compositions of zinc oxide doped Sodium Bismuth Borate glass, providing insights into the effects of varying zinc oxide concentrations on the glass system's radiation shielding properties.

### Mass Attenuation Coefficient (MAC)

The mass attenuation coefficient (MAC) for current glass samples is shown in Fig. 1 at low energy (0.015 MeV), the MAC values are the highest for all prepared glass samples, and the MAC values situated at 27.017, 35.330, 42.036, 47.560, and 52.190 cm<sup>2</sup>/g for ZNBB1, ZNBB2, ZNBB3, ZNBB4, and ZNBB5 glass samples, respectively. At high energy (10 MeV), the MAC values were lowest for all prepared specimens, and MAC values lie at 0.030, 0.027, and 0.022 cm<sup>2</sup>/g for ZNBB1, ZNBB2, ZNBB3, ZNBB4, and ZNBB5 glass samples as shown in Table 1 respectively. The studied samples show a gradual increase in MAC (Mass Attenuation Coefficient) that correlate with density, a trend also observe in other studies (M.H.A. Mhareb, 2020 and Sayyed, et al., 2020). In general, MAC values represent the total mass attenuation coefficient for photoelectric, Compton and pair production interactions. At low energies, photoelectric interaction dominates, contributing most significantly to the MAC value. In contrast, at the upper energy side, the photoelectric interaction reduces, and Compton and pair production increases gradually. In this work, adding zinc oxide and barium oxide to borate glass increases the glass sample's density gradually increasing the MAC values due to a higher probability of interaction between the incident photons and matter.

**Table 2: MAC Values of the  $x\text{ZnO}-(15-x)\text{Na}_2\text{O}-15\text{Bi}_2\text{O}_3-70\text{B}_2\text{O}_3$  Glass System obtained using Phy-X/PSD Software**

| Energy (MeV) | Mass Attenuation Coefficient ( $\text{m}^2/\text{kg}$ ) |        |        |        |        |
|--------------|---|--------|--------|--------|--------|
|              | ZNBB1   | ZNBB2  | ZNBB3  | ZNBB4  | ZNBB5  |
| 1.50E-02     | 27.017  | 35.330 | 42.036 | 47.560 | 52.190 |
| 2.00E-02     | 12.475  | 16.394 | 19.556 | 22.161 | 24.344 |
| 3.00E-02     | 4.236   | 5.577  | 6.658  | 7.549  | 8.296  |
| 4.00E-02     | 5.162   | 5.447  | 5.677  | 5.866  | 6.024  |
| 5.00E-02     | 2.933   | 3.086  | 3.209  | 3.311  | 3.396  |
| 6.00E-02     | 3.091   | 4.156  | 5.016  | 5.725  | 6.318  |
| 8.00E-02     | 1.512   | 2.017  | 2.425  | 2.760  | 3.042  |
| 1.00E-01     | 0.885   | 1.162  | 1.386  | 1.571  | 1.726  |
| 1.50E-01     | 0.371   | 0.463  | 0.537  | 0.598  | 0.649  |
| 2.00E-01     | 0.227   | 0.268  | 0.302  | 0.329  | 0.352  |
| 3.00E-01     | 0.138   | 0.151  | 0.162  | 0.171  | 0.178  |
| 4.00E-01     | 0.108   | 0.114  | 0.118  | 0.122  | 0.125  |
| 5.00E-01     | 0.093   | 0.095  | 0.098  | 0.100  | 0.101  |
| 6.00E-01     | 0.083   | 0.084  | 0.085  | 0.086  | 0.087  |
| 8.00E-01     | 0.070   | 0.071  | 0.071  | 0.071  | 0.071  |
| 1.00E+00     | 0.062   | 0.062  | 0.062  | 0.062  | 0.062  |
| 1.50E+00     | 0.050   | 0.050  | 0.050  | 0.050  | 0.049  |
| 2.00E+00     | 0.044   | 0.043  | 0.043  | 0.043  | 0.043  |
| 3.00E+00     | 0.037   | 0.037  | 0.037  | 0.037  | 0.037  |
| 4.00E+00     | 0.033   | 0.034  | 0.034  | 0.034  | 0.035  |
| 5.00E+00     | 0.031   | 0.032  | 0.033  | 0.033  | 0.034  |
| 6.00E+00     | 0.030   | 0.031  | 0.032  | 0.032  | 0.033  |
| 8.00E+00     | 0.028   | 0.030  | 0.031  | 0.032  | 0.033  |
| 1.00E+01     | 0.028   | 0.030  | 0.031  | 0.033  | 0.034  |
| 1.50E+01     | 0.028   | 0.031  | 0.033  | 0.034  | 0.036  |

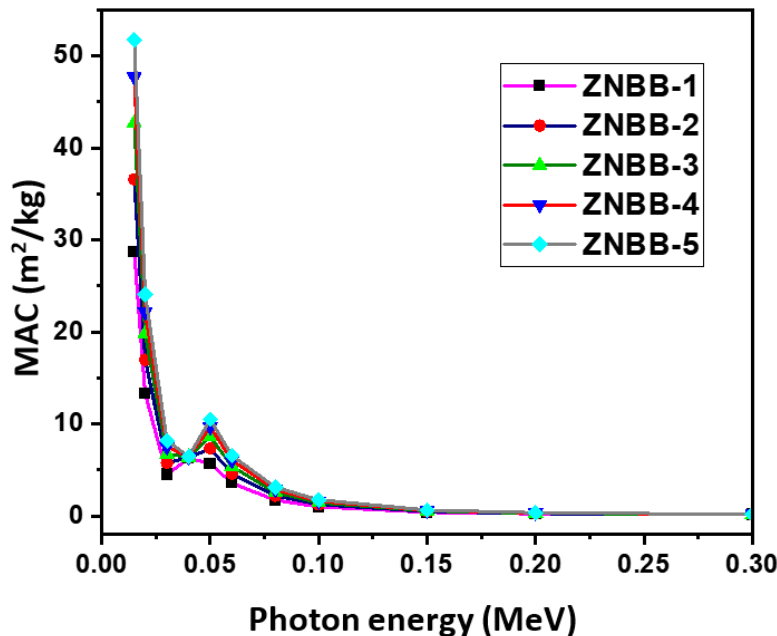


Figure 1: The Mass Attenuation Coefficient (MAC) of the Zinc Bismuth Borate Glasses Against Energy

**Linear Attenuation Coefficient (LAC)**

The variation of linear attenuation coefficient as shown in Fig.2 above for the ZNBB1, ZNBB2, ZNBB3, ZNBB4, and ZNBB5 at energies changing from 0.015 MeV to 10 MeV. This figure demonstrates a trend in  $\mu$  that is similar to those found for other glass systems, like borate glasses (Sayyed, et al 2018) and phosphate glasses (El-Taher et al., 2019). The Linear Attenuation Coefficient ( $\mu$ ) in Fig. 2 has a direct relationship with energy and has a highly large value (i.e. at 0.015 MeV). At this energy, the  $\mu$  takes the following values: 89.427, 139.552, 185.798, 233.521, and 272.954  $\text{cm}^{-1}$  for ZNBB1, ZNBB2, ZNBB3, ZNBB4, and ZNBB5. These high values in  $\mu$  at low energy may be demonstrated by the photoelectric mechanism, which has a strong effect at low photon energy zone. For this process, the cross section highly depends upon the atomic number, and the selected  $x\text{ZnO-(15-x) Na}_2\text{O-15Bi}_2\text{O}_3\text{-70B}_2\text{O}_3$  system

contains high atomic number elements (ZnO) which increase the likelihood of this process to take place. Generally, the  $\mu$  values presented in the Fig. 2 decreases as the energy increased. This trend causes all samples to have greater interactions with gamma photons at low energies, hence a higher photon attenuation efficiency that reduces as energy increases. Also, we can observe that the decreasing rate in  $\mu$  at low energy is very high, while it decreased at a smooth rate at higher energies. Inspecting the data presented in Table 3 carefully we can see that the  $\mu$  values increase as more ZnO is added in the glass series and it causes the increase in the density of the glass from 3.75 to 4.08  $\text{g.cm}^{-3}$ . We can conclude from linear attenuation coefficient curves that the ZNBB1-ZNBB5 glasses can effectively attenuate photons which possess low energies, and as photon energy increases, the attenuating ability of the samples decrease.

**Table 3: LAC Values of the  $x\text{ZnO-(15-x) Na}_2\text{O-15Bi}_2\text{O}_3\text{-70B}_2\text{O}_3$  Glass System Obtained using Phy-x/PSD Software**

| Energy (MeV) | Linear Attenuation Coefficient ( $\text{cm}^{-1}$ ) |         |         |         |         |
|--------------|---|---------|---------|---------|---------|
|              | ZNBB1   | ZNBB2   | ZNBB3   | ZNBB4   | ZNBB5   |
| 1.50E-02     | 89.427  | 139.552 | 185.798 | 233.521 | 272.954 |
| 2.00E-02     | 41.291  | 64.756  | 86.437  | 108.809 | 127.317 |
| 3.00E-02     | 14.021  | 22.028  | 29.430  | 37.067  | 43.388  |
| 4.00E-02     | 17.086  | 21.515  | 25.090  | 28.801  | 31.508  |
| 5.00E-02     | 9.709   | 12.190  | 14.185  | 16.257  | 17.761  |
| 6.00E-02     | 10.230  | 16.418  | 22.172  | 28.108  | 33.044  |
| 8.00E-02     | 5.005   | 7.968   | 10.717  | 13.554  | 15.908  |
| 1.00E-01     | 2.928   | 4.592   | 6.128   | 7.714   | 9.025   |
| 1.50E-01     | 1.229   | 1.828   | 2.373   | 2.935   | 3.393   |
| 2.00E-01     | 0.752   | 1.060   | 1.334   | 1.616   | 1.842   |
| 3.00E-01     | 0.457   | 0.598   | 0.716   | 0.838   | 0.932   |
| 4.00E-01     | 0.357   | 0.449   | 0.523   | 0.599   | 0.655   |
| 5.00E-01     | 0.306   | 0.377   | 0.432   | 0.489   | 0.529   |
| 6.00E-01     | 0.274   | 0.333   | 0.378   | 0.425   | 0.457   |
| 8.00E-01     | 0.232   | 0.279   | 0.314   | 0.350   | 0.374   |
| 1.00E+00     | 0.206   | 0.245   | 0.275   | 0.305   | 0.325   |
| 1.50E+00     | 0.166   | 0.197   | 0.219   | 0.243   | 0.258   |
| 2.00E+00     | 0.144   | 0.172   | 0.192   | 0.212   | 0.226   |
| 3.00E+00     | 0.121   | 0.145   | 0.164   | 0.183   | 0.195   |
| 4.00E+00     | 0.109   | 0.133   | 0.151   | 0.169   | 0.182   |
| 5.00E+00     | 0.102   | 0.126   | 0.144   | 0.163   | 0.176   |
| 6.00E+00     | 0.098   | 0.122   | 0.140   | 0.159   | 0.173   |
| 8.00E+00     | 0.094   | 0.118   | 0.138   | 0.158   | 0.173   |
| 1.00E+01     | 0.093   | 0.118   | 0.139   | 0.160   | 0.176   |
| 1.50E+01     | 0.094   | 0.121   | 0.144   | 0.168   | 0.187   |

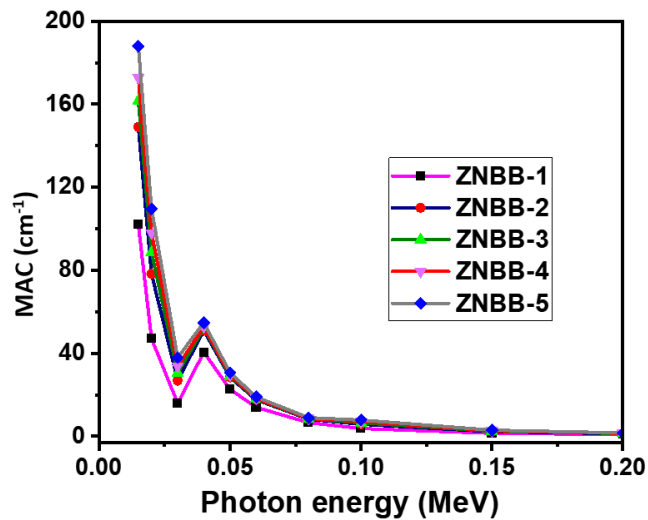


Figure 2: The Linear Attenuation Coefficient (LAC) of the Zinc Bismuth Borate Glasses against Energy

Previous studies have reported that transition metal ions (e.g.,  $V_2O_5$ ,  $CuO$ ,  $ZnO$ ,  $MoO_3$ , and  $WO_3$ ) glasses enhanced MAC and LAC (El Batal 2020). The MAC value obtained from this study has the better shielding ability in comparison to that reported in Borate glass  $Cu^{2+}/Zn^{2+}$  (Abou Hussein et al., 2021), phosphate glass (M. A. Alothman, 2021), Borate glass  $Sm_2O_3$  (Abouhaswa, et al., 2020) and commercial RS 253 (K. A. Mahmoud, 2020). However, the result of MAC is comparable to that of  $SiO_2$ - $MgO$  glass material (Alalawi, et al., 2023). This comparison suggests that  $ZnO$  added glasses have a superior attenuation capabilities, making them an excellent material for gamma shielding.

#### Half Value Layer

Fig.3 displays the HVL results for the ZNBB1, ZNBB2, ZNBB3, ZNBB4, and ZNBB5 glasses samples between 0.01 to 10 MeV. It was noticed that ZNBB5 sample has the shortest HVL values, then it increases with the reduction in zinc concentrations. Since a low HVL-values indicate the best radiation shielding of glass, the decline in HVL values with an increment of zinc contents could be correlated with the impact of zinc on shielding properties for prepared glass samples. The study conclude that the increase in density values for glass sample increases the probability of photon interaction and reduce the number of photon penetration through glass samples. Thus, the prepared glass samples show an excellent attenuation at lower energies, and this implies that glass samples is very useful at low energy.

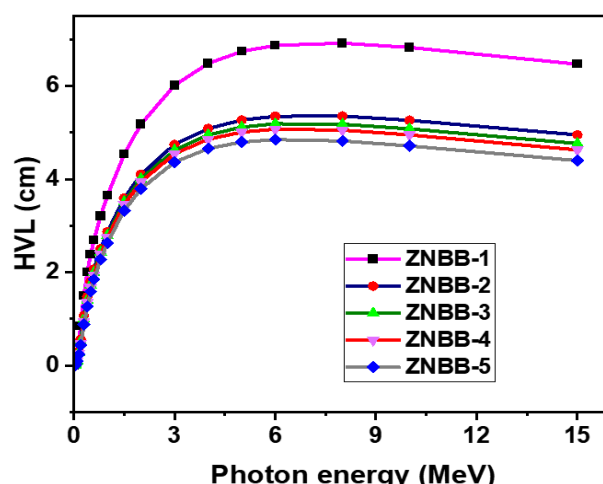


Figure 3: The Half Value Layer (HVL) of the Zinc Bismuth Borate Glasses against Energy

**Table 4: HVL Values of the xZnO-(15-x) Na<sub>2</sub>O-15Bi<sub>2</sub>O<sub>3</sub>-70B<sub>2</sub>O<sub>3</sub> Glass System Obtained using Phy-x/PSD Software**

| Energy (MeV) | Half value layer (cm) |       |       |       |       |
|--------------|-----------------------|-------|-------|-------|-------|
|              | ZNBB1                 | ZNBB2 | ZNBB3 | ZNBB4 | ZNBB5 |
| 1.50E-02     | 0.008                 | 0.005 | 0.004 | 0.003 | 0.003 |
| 2.00E-02     | 0.017                 | 0.011 | 0.008 | 0.006 | 0.005 |
| 3.00E-02     | 0.049                 | 0.031 | 0.024 | 0.019 | 0.016 |
| 4.00E-02     | 0.041                 | 0.032 | 0.028 | 0.024 | 0.022 |
| 5.00E-02     | 0.071                 | 0.057 | 0.049 | 0.043 | 0.039 |
| 6.00E-02     | 0.068                 | 0.042 | 0.031 | 0.025 | 0.021 |
| 8.00E-02     | 0.138                 | 0.087 | 0.065 | 0.051 | 0.044 |
| 1.00E-01     | 0.237                 | 0.151 | 0.113 | 0.090 | 0.077 |
| 1.50E-01     | 0.564                 | 0.379 | 0.292 | 0.236 | 0.204 |
| 2.00E-01     | 0.922                 | 0.654 | 0.520 | 0.429 | 0.376 |
| 3.00E-01     | 1.516                 | 1.159 | 0.968 | 0.827 | 0.744 |
| 4.00E-01     | 1.940                 | 1.544 | 1.326 | 1.156 | 1.058 |
| 5.00E-01     | 2.264                 | 1.840 | 1.605 | 1.417 | 1.310 |
| 6.00E-01     | 2.533                 | 2.084 | 1.835 | 1.632 | 1.517 |
| 8.00E-01     | 2.982                 | 2.484 | 2.210 | 1.982 | 1.855 |
| 1.00E+00     | 3.369                 | 2.824 | 2.524 | 2.273 | 2.134 |
| 1.50E+00     | 4.181                 | 3.520 | 3.158 | 2.852 | 2.685 |
| 2.00E+00     | 4.811                 | 4.041 | 3.619 | 3.263 | 3.067 |
| 3.00E+00     | 5.731                 | 4.767 | 4.235 | 3.794 | 3.547 |
| 4.00E+00     | 6.350                 | 5.225 | 4.602 | 4.095 | 3.807 |
| 5.00E+00     | 6.771                 | 5.515 | 4.820 | 4.262 | 3.942 |
| 6.00E+00     | 7.055                 | 5.696 | 4.945 | 4.349 | 4.005 |
| 8.00E+00     | 7.364                 | 5.859 | 5.030 | 4.386 | 4.013 |
| 1.00E+01     | 7.473                 | 5.877 | 5.004 | 4.336 | 3.947 |
| 1.50E+01     | 7.406                 | 5.713 | 4.797 | 4.114 | 3.715 |

**Tenth Value Layer**

In this work, the tenth value layer (TVL) for the xZnO-(15-x) Na<sub>2</sub>O-15Bi<sub>2</sub>O<sub>3</sub>-70B<sub>2</sub>O<sub>3</sub> is also presented, and the effect of ZnO with different concentrations is investigated. The lower the TVL, the less the material is needed to block the gamma photons to tenth of its original intensity. Using the Phy-X / PSD program, the TVL for ZBBN1- ZBBN5 glasses was evaluated for the investigated photon energy range, namely between 0.015 MeV to 10 MeV and we presented the results in Fig.4. Apparently from this figure and for all tested glasses, the TVL gradually increases as the energy varies from 0.015 to 10 MeV. The minimum TVL for the five tested glasses was found for gamma energy 0.015 MeV. For that particular energy, the TVL ranges between 0.008 cm for the ZBBN5 glass and 0.028 cm for the ZBBN1. Also, the

TVL curves imply that increasing the weight percentage of ZnO in the glasses from 0 to 12 mol% can reduce the thickness needed to attenuate or block the gamma photons. This is clearly observed from the curves since the TVL takes the order of ZBBN1> ZBBN2> ZBBN3> ZBBN4> ZBBN5 at all energies. Thus, the glass which contains the maximum content of ZnO, namely ZBBN5 has the lowest thickness and vice versa. This result is directly related to the density of the glass, where increasing the percentage of ZnO in the glass results in an overall increase of the density of the glass (as seen in Table 3. when the ZnO content changes from 0 to 12 mol%, the density changes from 3.75 to 4.08 g/cm<sup>3</sup>). The study concludes that as the density increase the TVL decreases, and therefore we can conclude that there is an increasing trend to shield more gamma photon.

**Table 5: TVL Values of the xZnO-(15-x) Na<sub>2</sub>O-15Bi<sub>2</sub>O<sub>3</sub>-70B<sub>2</sub>O<sub>3</sub> Glass System Obtained using Phy-x/PSD Software**

| Energy (MeV) | Ten value layer (cm) |        |        |        |        |
|--------------|----------------------|--------|--------|--------|--------|
|              | ZNBB1                | ZNBB2  | ZNBB3  | ZNBB4  | ZNBB5  |
| 1.50E-02     | 0.026                | 0.016  | 0.012  | 0.010  | 0.008  |
| 2.00E-02     | 0.056                | 0.036  | 0.027  | 0.021  | 0.018  |
| 3.00E-02     | 0.164                | 0.105  | 0.078  | 0.062  | 0.053  |
| 4.00E-02     | 0.135                | 0.107  | 0.092  | 0.080  | 0.073  |
| 5.00E-02     | 0.237                | 0.189  | 0.162  | 0.142  | 0.130  |
| 6.00E-02     | 0.225                | 0.140  | 0.104  | 0.082  | 0.070  |
| 8.00E-02     | 0.460                | 0.289  | 0.215  | 0.170  | 0.145  |
| 1.00E-01     | 0.786                | 0.501  | 0.376  | 0.299  | 0.255  |
| 1.50E-01     | 1.874                | 1.259  | 0.970  | 0.785  | 0.679  |
| 2.00E-01     | 3.062                | 2.171  | 1.726  | 1.425  | 1.250  |
| 3.00E-01     | 5.035                | 3.852  | 3.216  | 2.746  | 2.472  |
| 4.00E-01     | 6.444                | 5.129  | 4.405  | 3.842  | 3.515  |
| 5.00E-01     | 7.520                | 6.112  | 5.333  | 4.709  | 4.351  |
| 6.00E-01     | 8.413                | 6.921  | 6.096  | 5.423  | 5.041  |
| 8.00E-01     | 9.906                | 8.253  | 7.341  | 6.583  | 6.161  |
| 1.00E+00     | 11.192               | 9.382  | 8.386  | 7.551  | 7.090  |
| 1.50E+00     | 13.888               | 11.693 | 10.490 | 9.474  | 8.918  |
| 2.00E+00     | 15.983               | 13.425 | 12.021 | 10.838 | 10.189 |
| 3.00E+00     | 19.039               | 15.836 | 14.068 | 12.602 | 11.783 |
| 4.00E+00     | 21.095               | 17.358 | 15.289 | 13.602 | 12.646 |
| 5.00E+00     | 22.492               | 18.322 | 16.013 | 14.158 | 13.097 |
| 6.00E+00     | 23.438               | 18.923 | 16.427 | 14.447 | 13.306 |
| 8.00E+00     | 24.464               | 19.462 | 16.710 | 14.571 | 13.329 |
| 1.00E+01     | 24.826               | 19.524 | 16.623 | 14.404 | 13.111 |
| 1.50E+01     | 24.603               | 18.977 | 15.936 | 13.667 | 12.341 |

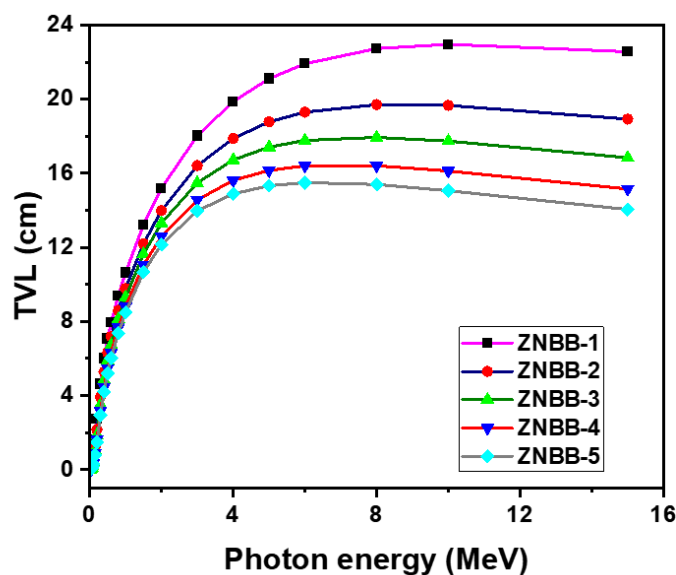


Figure 4: The Tenth Value Layer (TVL) of the Zinc Bismuth Borate Glasses against Energy

## CONCLUSION

The present work aimed to investigate the radiation shielding factors of  $x\text{ZnO}-(15-x)\text{Na}_2\text{O}-15\text{Bi}_2\text{O}_3-70\text{B}_2\text{O}_3$  glass system by employing Phy-X / PSD program. The effect of changing  $\text{ZnO}$  content from 0 to 12 mol% between 0.015MeV and 15MeV on the photons attenuation features of this glass system has been studied. The results show that introducing  $\text{ZnO}$  causes the increase in the density of the glass from 3.75 to 4.08 g/cm<sup>3</sup> which lead to increase the  $\mu$  and decrease TVL and HVL. The  $\mu$  has a direct relationship with energy and has a highly large value at 0.015MeV (between 27.017 and 52.190 cm<sup>-2</sup>). The TVL curves showed that increasing the weight percentage of  $\text{ZnO}$  in the glasses from 0 to 12 mol% can reduce the thickness needed to attenuate or block the photons. ZBBN5 is found to have the smallest HVL due to high amount of  $\text{ZnO}$  in this sample. Besides, the results revealed that as the density increased, the mean free path (MFP) gradually decreased, and the attenuation ability improves. The present work has provided the analysis and described the gamma radiation shielding properties of sodium bismuth borate glass.

## REFERENCES

A.S. Abouhaswa, M.I. Sayyed, Abeer S. Altowyan, Y. Al-Hadeethi, K.A. Mahmoud, "Synthesis, optical and radiation shielding capacity of the  $\text{Sm}_2\text{O}_3$  doped borate glasses" <https://doi.org/10.1016/j.jnoncrysol.2020.120505.19> October 2020

Al-Hadeethi, Y., & Sayyed, M. I. (2020). Using Phy-X/PSD to investigate gamma photons in  $\text{SeO}_2-\text{Ag}_2\text{O}-\text{TeO}_2$  glass systems for shielding applications. *Ceramics International*, 46(8), 12416–12421. <https://doi.org/10.1016/j.ceramint.2020.02.003>

A. Alalawi, M. Al Huwayz, Z. A. Alrowaili and M. S. Al-Buriahi, "Radiation attenuation of  $\text{SiO}_2-\text{MgO}$  glass system for shielding applications," *Journal of Radiation Research and Applied Sciences*, vol. 16(4), p. 100746, 2023.

Beir, V. (1990). Health effects of exposure to low levels of ionizing radiation. *Biological Effects of Ionizing Radiations*, 22–45. <https://doi.org/10.17226/1224>

E. M. Abou Hussein, F. I. El-Agawany, K. A. Mahmoud, Emad M. Ahmed, Abdelrahman A. Badawy, and Y. S. Rammah, "Radiation shielding, optical, and physical properties of alkali borate glasses modified with  $\text{Cu}^{2+}/\text{Zn}^{2+}$  ions", *J Mater Sci: Mater Electron* (2021) 32:19733–19741, <https://doi.org/10.1007/s10854-021-06497-y>. 7 July 2021

Erdem Şakara, Özgür Fırat Özpolatb, Bünyamin Alım, M.I. Sayyed, Murat Kurudirek "Phy-X / PSD: Development of a user-friendly online software for calculation of parameters relevant to radiation shielding and dosimetry", *Radiation Physics and Chemistry* 166 (2020) 108496, <https://doi.org/10.1016/j.radphyschem.2019.108496>. 24 September 2019

El-Agawany, F. I., Mahmoud, K. A., Kavaz, E., El-Mallawany, R., & Rammah, Y. S. (2020). Evaluation of nuclear radiation shielding competence for ternary Ge–Sb–S chalcogenide glasses. *Applied Physics A*, 126(4), 1–11. <https://doi.org/10.1007/s00339-020-3426-7>

Fatemah. H. Alkallas, Amira Ben Gouider Trabelsi, Samira Elaissi, Tahani A. Alrebdī, Lamia Abu El Maati, Fatma. B. M. Ahmed, M. M. Mahasen, M. Ahmad & M. M. Soraya (2022) Investigation of the gamma photon shielding in Se–Te–Ag chalcogenide glasses using the Phy-X/PSD software, *Cogent Engineering*, 9:1, 2116829, DOI: <https://doi.org/10.1080/23311916.2022.2116829>

Gokce, H. S., Yalcinkaya, C., & Tuyan, M. (2018). Optimization of reactive powder concrete by means of barite aggregate for both neutrons and gamma rays. *Construction and Building Materials*, 189, 470–477. <https://doi.org/10.1016/j.conbuildmat.2018.09.022>

J.M. An, H. Lin, E.Y.B. Pun, D.S. Li, "Synthesis, gamma and neutron attenuation capacities of boron-tellurite glass system utilizing Phy-X/PSD database" *Materials Chemistry and Physics* 274 (2021) 125166, <https://doi.org/10.1016/j.matchemphys.2021.125166> (2021)

K.A. Mahmoud, O.L. Tashlykov, M.I. Sayyed, E. Kavaz, The role of cadmium oxides in the enhancement of radiation shielding capacities for alkali borate glasses, *Ceramics International* (2020). <https://doi.org/10.1016/j.ceramint.2020.02.219>.

M. Y. Hassaan1, H. A. Saudi, Hossam M. Gomaa, Ammar S. Morsy, "Optical Properties of Bismuth Borate Glasses Doped with Zinc and Calcium Oxides" *Journal of Materials and Applications* 2020;9(1):46-54. <https://doi.org/10.32732/jma.2020.9.1.46> (15 May 2020)

M.H.A. Mhareba, Muna Alqahtania, Fatimh Alshahria, Y.S.M. Alajeramic, Noha Saleha, N. Alonizana, M.I. Sayyede, M.G.B. Ashiqa, Taher Ghriba, Sarah Ibrahim Al-Dhafar, Tasneem Alayed, Mohamed A. Morsy "The impact of barium oxide on physical, structural, optical, and shielding features of sodium zinc borate glass", *Journal of Non-Crystalline Solids* 541 (2020) 120090,

<https://doi.org/10.1016/j.jnoncrysol.2020.120090> 31  
March 2020

M.I. Sayyed, M.H.A. Mhareb, Y.S.M. Alajerami, K.A. Mahmoud, Mohammad A. Imheidat, Fatimah Alshahri, Muna Alqahtani, T. Al-Abdullah "Optical and radiation shielding features for a new series of borate glass samples", International Journal for Light and Electron Optics 239 (2021) 166790, <https://doi.org/10.1016/j.ijleo.2021.166790>. 17 March 2021

M. A. Alothman, Z. A. Alrowaili, A. M. Al-Baradi, O. Kilicoglu, C. Mutuwong and M. S. Al-Buriahi, "Elastic properties and radiation shielding ability of ZnO-P2O5/B2O3 glass system," *Journal of Materials Science: Materials in Electronics*, vol. 32(14), pp. 19203-19217, DOI: <https://doi.org/10.1007/s10854-021-06442-z> 2021.

M.H.A. Mhareb, Physical, optical and shielding features of Li<sub>2</sub>O-B<sub>2</sub>O<sub>3</sub>-MgO-Er<sub>2</sub>O<sub>3</sub> glasses co-doped of Sm<sub>2</sub>O<sub>3</sub>, *Appl. Phys. A* 126 (1) DOI: <https://doi.org/10.1007/s00339-019-3262-9>(2020)71-79.

M.I. Sayyed, et al., Bi<sub>2</sub>O<sub>3</sub>-B<sub>2</sub>O<sub>3</sub>-ZnO-BaO-Li<sub>2</sub>O glass system for gamma ray shielding applications, *Optik* (Stuttg) 201

<https://doi.org/10.1016/j.ijleo.2019.163525>(2020)163525.

M.I. Sayyed, B.O. Elbashir, H.O. Tekin, E.E. Altunsoy, D.K. Gaikwad, Radiation shielding properties of pentaternary borate glasses using MCNPX code, *Journal of Physics and Chemistry of Solids* 121 DOI: <https://doi.org/10.1016/j.jpcs.2018.05.009>(2018)17-21

R. Divinaa, G. Sathiyapriyaa, K. Marimuthua, A. Askinb, M.I. Sayyedc, "Structural, elastic, optical and  $\gamma$ -ray shielding behavior of Dy<sup>3+</sup> ions doped heavy metal incorporated borate glasses" *Journal of Non-Crystalline Solids* 545 (2020) 120269, <https://doi.org/10.1016/j.jnoncrysol.2020.120269>, 24 June 2020

Salama, Elsayed; Maher, Abeer; and Youssef, Gamal, "Gamma Radiation and Neutron Shielding Properties of Transparent Alkali Borosilicate Glass Containing Lead". *Basic Science Engineering*. 1. [https://buescholar.bue.edu.eg/basic\\_sci\\_eng/1](https://buescholar.bue.edu.eg/basic_sci_eng/1) (2019)

Y. Al-Hadeethi, et al., Fabrication, optical, structural and gamma radiation shielding characterizations of GeO<sub>2</sub>-PbO-Al<sub>2</sub>O<sub>3</sub>-CaO glasses, *Ceram. Int.* 46 DOI: <https://doi.org/10.1016/j.ceramint.2019.09.185>(2020)2055-2062.